HUMAN GENE THERAPY METHODS 24:372–380 (December 2013)

DOI: 10.1089/hgtb.2013.124

Adeno-Associated Virus Enhances Wild-Type and Oncolytic Adenovirus Spread

Eduardo Laborda,[1,2] Cristina Puig-Saus,[1] Manel Cascalló,[3] Miguel Chillón,[2,4] and Ramon Alemany[1]

Abstract

The contamination of adenovirus (Ad) stocks with adeno-associated viruses (AAV) is usually unnoticed, and it has been associated with lower Ad yields upon large-scale production. During Ad propagation, AAV contamination needs to be detected routinely by polymerase chain reaction without symptomatic suspicion. In this study, we describe that the coinfection of either Ad wild type 5 or oncolytic Ad with AAV results in a large-plaque phenotype associated with an accelerated release of Ad from coinfected cells. This accelerated release was accompanied with the expected decrease in Ad yields in two out of three cell lines tested. Despite this lower Ad yield, coinfection with AAV accelerated cell death and enhanced the cytotoxicity mediated by Ad propagation. Intratumoral coinjection of Ad and AAV in two xenograft tumor models improved antitumor activity and mouse survival. Therefore, we conclude that accidental or intentional AAV coinfection has important implications for Ad-mediated virotherapy.

Introduction

Oncolytic viruses offer a unique opportunity to treat cancer because selective replication in tumor cells multiplies the amount of cells that become infected, a major limitation in cancer gene therapy. Among different viruses, adenovirus (Ad) has been extensively modified to achieve tumor selective replication (Alemany, 2007). However, despite promising preclinical results, limited efficacy in over 20 clinical trials suggests that Ad oncolytic potency needs to be improved (Russell *et al.*, 2012). A potent oncolytic Ad should efficiently release its progeny to facilitate rapid spread through the tumor. Despite that Ad release is key for efficient oncolysis (Gros, 2010), it is slow, as it occurs late in the virus life cycle when the adenovirus death protein (ADP) has accumulated (Tollefson *et al.*, 1996b). Moreover, Ad release is inefficient, as less than 20% of the total virus produced is released within 2 days postinfection. Mathematical models that combine parameters of Ad replication rate, tumor growth rate, and immune response point to virus release as a key factor for efficacy (Wein *et al.*, 2003). Ads with deleted *E1B19K*, truncated i-leader protein, or overexpressing ADP show faster progeny release and higher oncolytic activity (Sauthoff *et al.*, 2000; Ramachandra *et al.*, 2001; Doronin *et al.*, 2003; Puig-Saus *et al.*, 2012), highlighting Ad release as a key parameter for intratumor spread and antitumor efficacy.

Adeno-associated viruses (AAVs) were first described in 1965 as nonautonomous viruses contaminating Ad stocks. AAVs are nonpathogenic defective parvoviruses. The name "AAV" reflects the inability to efficiently replicate in the absence of a helper virus, such as Ad, human papilomavirus or herpes simplex virus. Several AAV serotypes have been described (Gao *et al.*, 2004; Schmidt *et al.*, 2006) with different tissue tropism (Grimm *et al.*, 2003; Muller *et al.*, 2006). Studies on AAV-Ad interaction frequently involve AAV2 and Ad wild type 2 (Ad 2) or Ad wild type 5 (Ad5). AAV2-Ad coinfection leads to lower levels of Ad gene and protein expression in an AAV dose-dependent manner, affecting certain Ad transcripts and proteins more than others (Timpe *et al.*, 2006). AAV contamination has been associated with lower Ad yields (burst size) (Hoggan *et al.*, 1966; Carter *et al.*, 1979). However, the effect of AAV contamination on Ad cytotoxicity is unclear, with a lower cytotoxicity described in HeLa cells (Jing *et al.*, 2001) and an enhanced cytolysis and apoptosis in A549 cells (Timpe *et al.*, 2007).

Considering the previously described effects of AAV on Ad yield and cytotoxicity and the current interest on virotherapy with Ads, we studied the effect of AAV on Ad

[1]Translational Research Laboratory, IDIBELL-Institut Català d'Oncologia, L'Hospitalet de Llobregat, 08907 Barcelona, Spain.
[2]Department of Biochemistry and Molecular Biology, Autonomous University of Barcelona, 08193 Barcelona, Spain.
[3]VCN Biosciences, Sant Cugat del Vallès, 08174 Barcelona, Spain.
[4]Center of Animal Biotechnology and Gene Therapy and Institut Català de Recerca i Estudis Avançats, 08193 Barcelona, Spain.

release, cytotoxicity, and oncolytic potency. Ad formed large plaques when combined with either AAV2 or AAV6, a phenotype caused by a faster and more efficient Ad release from infected cells. Of note, AAV also enhanced cell death and improved therapeutic activity of an oncolytic Ad, opening the possibility to use AAV in Ad-mediated virotherapy.

Materials and Methods

Cell lines and viruses

HEK293 and A549 cells were obtained from the American Type Culture Collection (ATCC, Manassas, VA). NP9 cells were established in our laboratory (Villanueva *et al.*, 1998). All cell lines were routinely tested for mycoplasma and were grown in Dulbecco's modified Eagle's medium (DMEM) supplemented with 5% fetal bovine serum (FBS), penicillin (50 mg/ml), and streptomycin (50 mg/ml) at 37°C and 5% CO_2. Human Ad5 was obtained from ATCC. Oncolytic Ad ICOVIR15 is described elsewhere (Rojas *et al.*, 2010). AAV serotype 2 was generated by transfection of HEK293 monolayers with psub201 and a plasmid supplying helper genes as previously described (Casper *et al.*, 2005). AAV serotype 6 was generated by pAAV6 (kindly provided by Dr. David W. Russell, Department of Medicine, University of Washington, Seattle, WA) and helper plasmid transfection of HEK293. AAV6 was purified over iodixanol gradient as described (Zolotukhin *et al.*, 1999). AAVs were tittered by quantitative polymerase chain reaction.

Cell-plaque assay

A549 monolayers were infected with Ad5 or ICOVIR15 at a multiplicity of infection (MOI) of 50, or coinfected with either Ad5 or ICOVIR15 (50 MOI) plus either AAV2 or AAV6 at 1,000 viral particles (vp)/cell. Four hours postinfection, cells were washed with phosphate buffered saline (PBS) and trypsinized. About 20 μl of each cell suspension was diluted 1/5 in trypan blue, and cells were counted in a Neubauer chamber. Fifty cells of each infection condition were added on top of near-confluent A549 monolayers seeded in six-well plates. After 4 hr, the medium was removed and cells were covered with a 1:1 mix of DMEM–5% FBS:1% agarose. Once agarose solidified, DMEM–5% FBS was added. To better visualize plaques, monolayers from the different infection conditions were stained by incubation with 0.5 mg/ml thiazolyl blue tetrazolium bromide (MTT; Sigma-Aldrich, St. Louis, MO) at 37°C and 5% CO_2 for 4 hr.

Virus release and production assays

HEK293, A549, and NP9 monolayers seeded in 24-well plates were infected in triplicate at an Ad MOI that allowed 100% infectivity (5 for HEK293; 50 for A549 and NP9 cells) and at different vp/cell of AAV6 depending on the cell line (100 for HEK293; 100, 1,000, 10,000, and 100,000 for A549; and 1,000 for NP9). Four hours after infection, cultures were washed thrice with PBS and incubated in a fresh virus-free medium. At the indicated time points after infection (time 0 meaning immediately after addition of the fresh medium), a small fraction of the supernatant (SN) was collected, and the cells and the medium were harvested and frozen-thawed three times to obtain the cell extract (CE). Viral titers were determined by an antihexon staining-based method (Cascallo *et al.*, 2007). A two-tailed Student's *t*-test was used to study statistical significance.

Cytotoxicity assays

A549 monolayers seeded in six-well plates were mock-infected or infected with ICOVIR15 (50 MOI) alone or combined with AAV6 at 1,000 vp/cell. Four hours postinfection, cells were washed thrice with PBS and incubated with fresh virus-free DMEM–5% FBS at 37°C and 5% CO_2. At the indicated time points, samples were collected and analyzed for lactate dehydrogenase (LDH) levels (expressed in uKAt/liter) in the Biochemistry Service of the Bellvitge Hospital following the protocol established by the International Federation of Clinical Chemistry. The absorbances at 340 and 700 nm were determined for each sample on a Cobas c711 (Roche Diagnostics, Basel, Switzerland) spectrophotometer, calibrated with a c.f.a.s. (Roche Diagnostics, ref. 759350) using reagent LDH 1 Gen. 2 (Roche Diagnostics, ref. 04964560 022). The significance of differences between groups was assessed by a two-tailed Student's unpaired *t*-test. For the trypan blue exclusion assay, SNs were removed at the indicated time points. Cells were trypsinized and combined with SNs. Cell and SN mixture was diluted 1/10 in trypan blue, and cells were counted in a Neubauer chamber. Cells were counted in groups of 100 (500–600 cells for each time point and condition). Statistical significance between groups was assessed by a two-tailed Student's unpaired *t*-test. For cell morphology, unfixed cells were microscopically examined and photographed at the indicated time points postinfection with a Leica DMIL LED light microscope and Leica Application Suite LAS v.2.6 software (Leica, Wetzar, Germany).

In vitro *propagation assays*

Propagation assays were performed by seeding 30,000 A549 or NP9 cells per well in 96-well plates in DMEM–5% FBS. Cells were infected by triplicate with serial dilutions of ICOVIR15 alone, starting with 200 transducing units (TU)/cell, or coinfected with four AAV6 doses, starting with 400, 4,000, 40,000, or 400,000 vp/cell for A549 or NP9 cells. These doses were chosen to match the number of functional AAV and Ad particles considering an Ad dose of 200 MOI and a similar TU/vp ratio for both viruses; thus, we used 4,000 vp of AAV. We used one lower dose and two higher doses in order to demonstrate a dose-dependent effect of AAV on Ad propagation-mediated citotoxicity. At day 5 postinfection for A549 cells and day 6 postinfection for NP9 cells, plates were washed with PBS and stained for total protein content (bicinchoninic acid assay; Pierce Biotechnology, Rockford, IL). Absorbance was quantified and the TU per cell required to produce 50% of culture growth inhibition (IC_{50} value) was estimated from dose–response curves by standard nonlinear regression (GraFit; Erithacus Software, Horley, United Kingdom), using an adapted Hill equation. A two-tailed Student's *t*-test was used to study the statistical differences between the IC_{50} values of different groups. For assays using coinfected cells, monolayers of A549 or NP9 cells were infected with ICOVIR15 alone (50 MOI) or combined with 1,000 vp/cell of AAV6. Four hours postinfection, cells were washed once with PBS, trypsinized, and counted in a Neubauer chamber. Serial dilutions of infected cells, starting with

1,000 A549 cells or 3,000 NP9 cells, were done by triplicate on 96-well plates and 30,000 A549 or NP9 noninfected cells were added, respectively. At day 7 for A549 cells and day 9 for NP9 cells, the same protocol of total protein staining, quantification, and statistical study as above was performed. In this case, IC_{50} values were calculated as the number of infected cells needed to produce 50% of culture growth inhibition.

In vivo *antitumoral efficacy*

Animal studies were performed at the IDIBELL animal facility (AAALAC unit 1155) and approved by the IDIBELL's Ethics Committee for Animal Experimentation. Subcutaneous A549 or NP9 carcinoma tumors were established by injection of 1.5×10^6 or 3×10^6 cells, respectively, into the flanks of 6-week-old female Balb/C *nu/nu* mice (Harlan Laboratories, Venray, B.V. Netherlands). To minimize the number of animals used, each animal was implanted with two tumors, one in each flank. When tumors reached 150 mm^3 (experimental day 0; $n=8$–10 tumors), mice were randomized and were injected with a single intratumor injection of PBS, 2×10^{10} vp of AAV6, 2×10^9 vp of ICOVIR15, or 2×10^{10} vp of AAV6 and 2×10^9 vp of ICOVIR15 in a volume of 20 μl in PBS. Tumor volume was defined by the equation, $V\ (mm^3)=\pi/6\times W^2\times L$, where W and L are the width and the length of the tumor, respectively. Data are expressed as relative tumor size to the beginning of the therapy. The statistical differences in relative tumor size between treatment groups were assessed by a two-tailed Student's unpaired *t*-test. For Kaplan–Meier survival curves, the end point was established at $\geq 500\ mm^3$. The survival curves from the different treatments were compared. Animals whose tumor size never achieved the threshold were included as right-censored information. A log-rank test was used to determine the statistical significance of the differences in time-to-event.

Results

Ad-AAV coinfection results in a large-plaque phenotype

We performed a cell-plaque assay to compare the plaque phenotypes of cells infected with Ad alone or Ad and AAV. We infected A549 cells with Ad5 or ICOVIR15 (Rojas *et al.*, 2010), each of them either alone or combined with AAV2 or AAV6. Fifty cells from each infection condition were added on top of near-confluent A549 monolayers and were covered with agarose to force the viruses to spread from cell to cell. Plaques derived from cells coinfected with Ad and either AAV2 or AAV6 appeared earlier and had a larger size at any given time point, for both Ad5 (Fig. 1a) and ICOVIR15 (Fig.

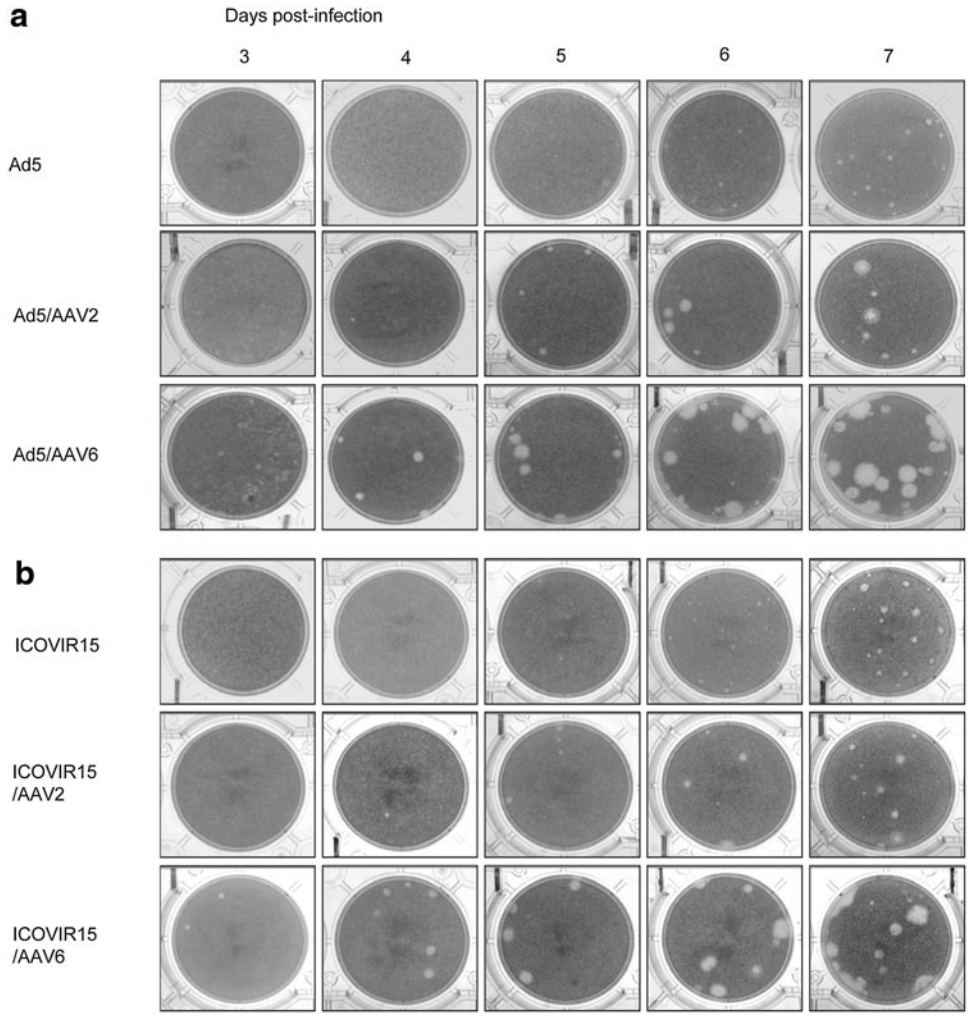

FIG. 1. Ad-AAV coinfection enlarges plaque size. Cell plaque assay of A549 cells infected with **(a)** Ad5 or **(b)** ICOVIR15 alone or combined with either AAV2 or AAV6. Fifty infected cells of each infection condition were added on top of A549 fresh monolayers previously seeded in six-well plates. Cell plaques were stained with MTT and photographed at the indicated time points. AAV, adeno-associated viruses; Ad, adenovirus.

1b). Interestingly, cells coinfected with AAV6 developed faster and larger plaques than AAV2; thus, we focused on AAV6.

Coinfection with AAV6 enhances ICOVIR15 release but decreases burst size

ICOVIR15 yield and release in the presence or absence of AAV6 were quantified in three cell lines (Fig. 2). HEK293 (human embryonic kidney) are commonly used to propagate Ads. A549 (lung adenocarcinoma) and NP9 (pancreatic adenocarcinoma) are tumor cell lines commonly used as models in virotherapy. Cells were synchronically infected with ICOVIR15 alone or combined with AAV6. At the indicated time points, SNs and CEs were harvested and Ad was tittered using an antihexon staining-based method (Cascallo *et al.*, 2007). In HEK293 cells (Fig. 2a), AAV6 increased ICOVIR15 release 10-, 15-, and 7-fold at 24, 48, and 72 hr postinfection, respectively ($p < 0.05$), but decreased 1.87- and 2.17-fold ICOVIR15 total production at 48 and 72 hr postinfection, respectively ($p < 0.05$). In A549 cells (Fig. 2b), coinfection with AAV6 increased ICOVIR15 release 87-, 34-, and 2.5-fold at 24, 48, and 72 hr postinfection, respectively ($p < 0.05$), but decreased total production 1.6-, 4.7-, and 6.75-fold at 24, 48, and 72 hr postinfection, respectively ($p < 0.05$). In NP9 cells (Fig. 2c), AAV6 enhanced ICOVIR15 release 13- and 5-fold compared with ICOVIR15 at 48 and 72 hr postinfection, respectively ($p < 0.05$). Total production was not affected in NP9 cells. A similar enhanced Ad release and lower Ad production was observed when infecting A549 cells with Ad5 and AAV6 (Supplementary Fig. S1; Supplementary Data are available online at

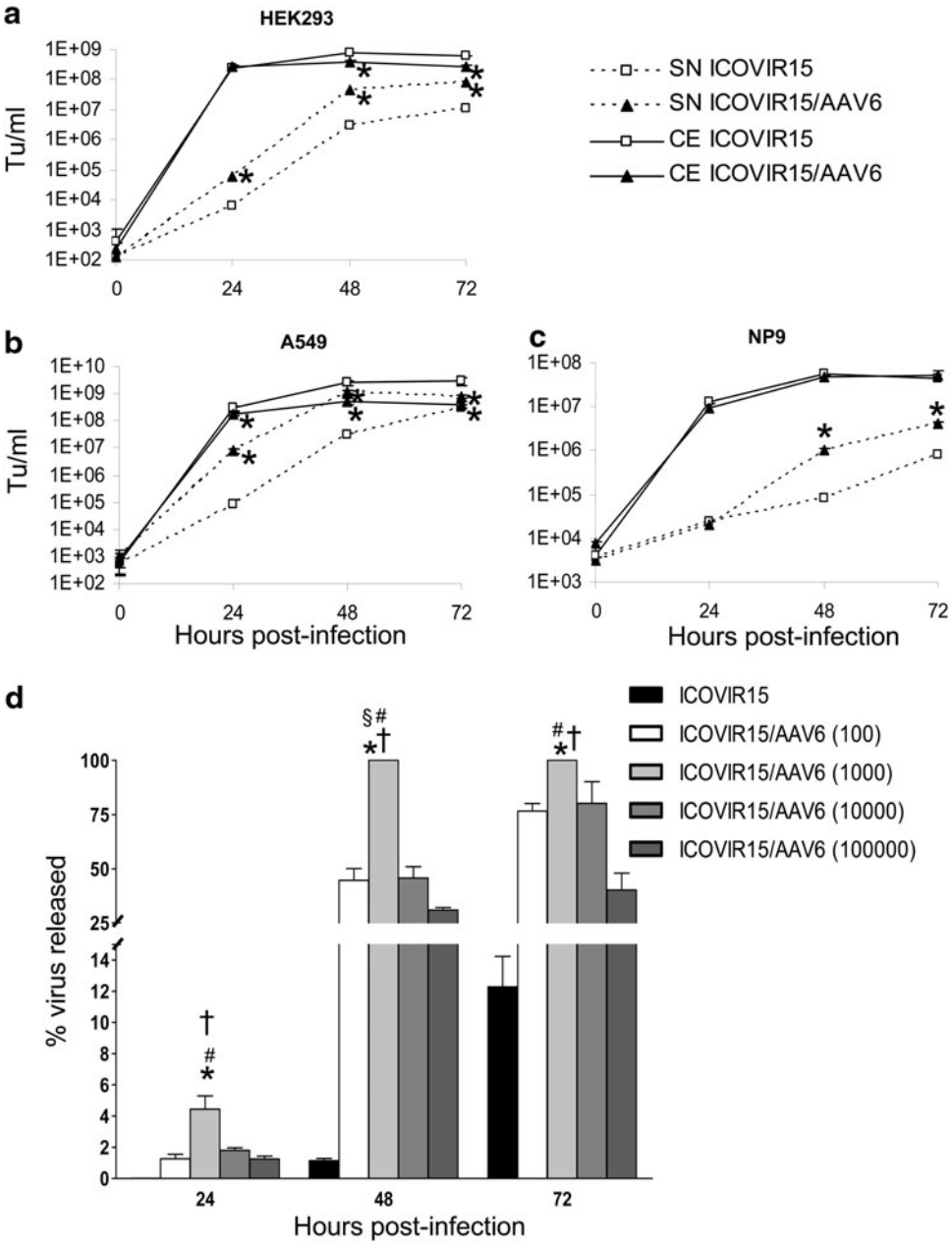

FIG. 2. Ad-AAV coinfection enhances Ad release. Viral production and release kinetics of ICOVIR15 alone or combined with AAV6 in **(a)** HEK293, **(b)** A549, and **(c)** NP9 cells. Extracellular (SN, supernatant) and total (CE, cell extract) Ad contents were analyzed at the time points indicated. Mean values ($n = 3$) ± SD are plotted. *$p \leq 0.05$ by two-tailed unpaired Student's *t*-test compared with ICOVIR15. **(d)** Percentage of viral release ([virus released/virus produced] × 100) in A549 cells infected with ICOVIR15 (50 MOI) alone or combined with AAV6 (100, 1,000, 10,000, and 100,000 vp/cell) at the indicated time points. Each bar indicates the average of three samples ($n = 3$) ± SD. *$p \leq 0.05$ compared with ICOVIR15, $^{\#}p \leq 0.05$ compared with ICOVIR15/AAV6 (100), $^{\S}p \leq 0.05$ compared with ICOVIR15/AAV6 (10,000), $^{\dagger}p \leq 0.05$ compared with ICOVIR15/AAV6 (100,000). MOI, multiplicity of infection.

www.liebertonline.com/hgtb). No differences of Ad content in total CE at time point 0 were observed in any cell line (Supplementary Fig. S2).

We extended the study on AAV6 effects on ICOVIR15 release and total production by coinfecting A549 cells with different AAV6 doses. We measured the relative amounts of Ad released (virus released/total virus produced) using four AAV6 doses (100, 1,000, 10,000, and 100,000 vp/cell) to find which dose enhanced ICOVIR15 release more efficiently (Fig. 2d). In all the time points analyzed, the dose of 1,000 vp/cell induced the highest relative Ad release. This dose was also the dose that induced the highest absolute amounts of virus released (Supplementary Fig. S3).

The viability of ICOVIR15-infected cells is reduced by AAV6

To detect morphology changes at early times associated to AAV6 coinfection, A549 cells were infected with ICOVIR15 alone or ICOVIR15 and AAV6. As described (Timpe *et al.*, 2007), coinfected cells showed an apoptotic-like morphology characterized by cell shrinkage and membrane blebbing as soon as 36 hr postinfection (Fig. 3a). Cells infected with ICOVIR15 alone showed minimal signs of cytopathic effect at the same time point (36 hr), but complete cytopathic effect at 72 hr postinfection. To further study this accelerated cell death, we studied plasma membrane integrity and cell lysis

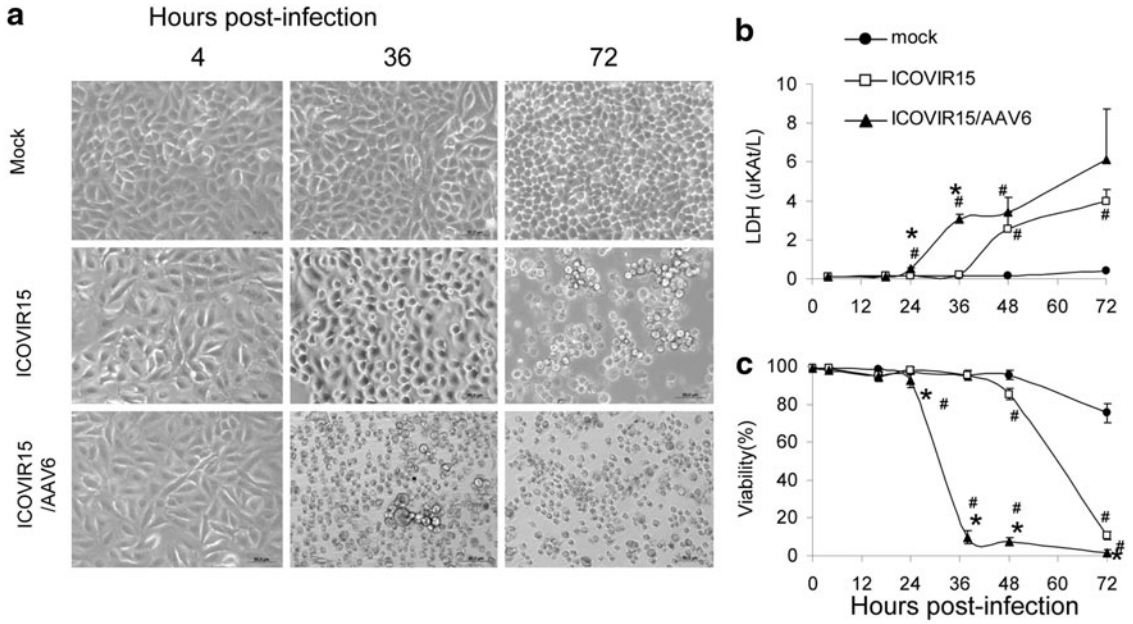

d

IC_{50}	ICOVIR15	ICOVIR15/AAV6 400	ICOVIR15/AAV6 4000	ICOVIR15/AAV6 40000	ICOVIR15/AAV6 400000
A549	0.07±0.007	0.015±0.002*	0.014±0.002*	0.006±0.001*	0.002±0.001*
NP9	0.908±0.111	0.275±0.017*	0.118±0.009*	0.069±0.003*	0.062±0.005*

e

IC_{50}	Cells infected with ICOVIR15	Cells infected with ICOVIR15/AAV6
A549	12.425±1.959	0.961±1.121 *
NP9	1002.677±188.291	72.12±15.664 *

FIG. 3. AAV6 coinfection induces cell shrinkage, accelerates cell death, and enhances ICOVIR15 propagation in ICOVIR15-infected cells. A549 cells were mock-infected or infected with ICOVIR15 (50 MOI) alone or combined with AAV6 (1,000 vp/cell). **(a)** Cell morphology at the indicated hours postinfection. **(b)** Cell lysis measured by LDH release into the culture medium. Mean values ($n=3$) ± SD are plotted. **(c)** Percentage of viable cells determined on the basis of exclusion of trypan blue from the cell. Mean values ($n=3$) ± SD are plotted. $^{\#}p \le 0.05$ by two-tailed unpaired Student's *t*-test compared with mock-infected cells, $^{*}p \le 0.05$ by two-tailed unpaired Student's *t*-test compared with ICOVIR15-infected cells. **(d)** The IC_{50} (ICOVIR15 TU/cell needed to cause a reduction of 50% in cell culture viability) values obtained from comparative dose–response curve of ICOVIR15 alone or combined with AAV6 (400, 4,000, 40,000, and 400,000 vp/cell) in A549 and NP9 cells. At day 5–6 postinfection, plates were washed with PBS and stained for total protein content. Three different replicates were quantified for each cell line. Mean ± SD are showed. $^{*}p \le 0.05$ by two-tailed unpaired Student's *t*-test compared with ICOVIR15. **(e)** The IC_{50} values (infected cells needed to cause a reduction of 50% in cell culture viability) obtained from comparative dose–response curve of A549 or NP9 cells infected with ICOVIR15 alone or combined with AAV6 at day 7–8 after infection are shown. Three different replicates were quantified for each cell line. Mean ± SD are shown. $^{*}p \le 0.05$ by two-tailed unpaired Student's *t*-test compared with cells infected with ICOVIR15.

using the same coinfection conditions. Cell lysis, measured by LDH release, showed a marked increase ($p < 0.01$) in coinfected cells compared with ICOVIR15-alone infected cells at early times (24 and 36 hr postinfection) (Fig. 3b). At later times (48 and 72 hr postinfection), lysis was not significantly different compared with ICOVIR15-infected cells. LDH levels in noninfected cells remained basal during all the experiment. Plasma membrane integrity and cell viability were monitored by trypan blue exclusion (Fig. 3c). Loss of membrane integrity and cell viability of coinfected cells appeared as soon as 24 hr postinfection. A minority of cells were viable 36 hr postcoinfection with ICOVIR15 and AAV6 (9.8%, 7.7%, and 1.7% of cells were viable at 36, 48, and 72 hr postcoinfection, respectively). In contrast, the majority of cells were viable at 36 and 48 hr postinfection with ICOVIR15 (95% and 85%, respectively). Viability was 11-fold higher for ICOVIR15-alone infected cells compared with coinfected cells (85.3% vs. 7.7%, $p < 0.01$) at 48 hr postinfection. Noninfected cell viability remained near 100% during all the experiment.

AAV6 enhances the ICOVIR15 propagation-mediated cytotoxicity in vitro

Cell monolayers were infected with low doses of viruses (achieved by serial dilutions) and incubated for several days to allow multiple rounds of replication. Such propagation-mediated cytotoxicity assays (IC_{50} assays; IC_{50}, amount of virus needed to reduce cell culture viability by 50%) were performed by infecting preseeded monolayers of A549 or NP9 cells with viruses or by seeding infected cells over them. To prepare virus mixtures, four initial different doses of AAV6 (400, 4,000, 40,000, and 400,000 vp/cell) and one initial dose of ICOVIR15 (200 transducing units [TU]/cell) were used. The results showed that AAV6 enhanced dose dependently the propagation-mediated cytotoxicity of ICOVIR15 (lower IC_{50} values) in both cell lines (Fig. 3d). Similar results were obtained when seeding monolayers with serial dilutions of cells infected with ICOVIR15 or ICOVIR15 and AAV6. Coinfection strongly enhanced cytotoxicity in both cells lines, decreasing dramatically the IC_{50} values (Fig. 3e). Comparative dose–response curves from both assays are shown in Supplementary Fig. S4.

ICOVIR15-AAV6 injection enhances antitumor activity and prolongs mice survival after intratumor administration

Once we had demonstrated the ICOVIR15-AAV6-enhanced cytotoxicity *in vitro*, we wanted to determine whether it conferred a therapeutic advantage *in vivo*. Mice bearing A549 or NP9 tumors were treated intratumorally with PBS, AAV6 (2×10^{10} vp/tumor), ICOVIR15 (2×10^{9} vp/tumor), or a mixture of ICOVIR15 and AAV6 at these same doses in a single injection (Fig. 4a). The AAV6 dose was 10-fold higher than the dose of ICOVIR15 to increase tumor cell coinfection probability. In the A549 model, coinjection reduced tumor growth compared with PBS- and AAV6-injected groups from day 14 postinjection (p.i.) ($p < 0.05$) until day 38 of treatment, when PBS and AAV6 groups had to be sacrificed because of uncontrolled tumor growth. ICOVIR15 reduced tumor growth compared with AAV6 at days 35 and 38 after treatment ($p < 0.05$). Coinjection reduced 2.6-fold the tumor growth compared with ICOVIR15 injection at the end of the experiment (day 66), although this difference was not statistically significant. In the NP9 model, the combination of both viruses resulted in a marked inhibition of tumor growth. ICOVIR15-AAV6 coinjection decreased tumor growth compared with control groups (PBS and AAV6) from day 20 p.i. ($p < 0.05$) and compared with ICOVIR15 from day 29 p.i. ($p < 0.05$). At the end of the study (day 48 after treatment), coinjection inhibited tumor growth 1.9-fold compared with ICOVIR15. Kaplan–Meier analysis (Fig. 4b) showed a survival benefit for the group treated with both viruses compared with controls in A549 and NP9 models ($p < 0.05$), and compared with ICOVIR15 group in NP9 model ($p < 0.05$). ICOVIR15 treatment showed a trend to improve the mean survival compared with control groups (PBS and AAV6) in both models although did not achieve statistical significance.

In summary, our results indicate that Ad coinfection with AAV induces a large-plaque phenotype caused by an increase in Ad release, which enhances Ad cytotoxicity *in vitro* and antitumor efficacy *in vivo*.

Discussion

A clear phenotype associated to AAV contamination of Ad stocks is the lower Ad production yield (Hoggan *et al.*, 1966; Carter *et al.*, 1979; Timpe *et al.*, 2006). As Ad, human papiloma virus (HPV) can also function as an AAV helper, and lower HPV yields have also been observed after AAV coinfection. Intriguingly, it has been described that AAV accelerates the HPV life cycle (Agrawal *et al.*, 2002). Here we describe that the combination of Ad5 or oncolytic Ad ICOVIR15 with either AAV2 or AAV6 results in earlier and larger-plaque phenotype. This phenotype is long-lived (14 days postinfection; not shown), suggesting an improvement in propagation that is sustained during multiple replication rounds. As a large-plaque phenotype correlates with enhanced antitumor activity of oncolytic Ads, we attempted to elucidate if the AAV-induced large-plaque phenotype could be applied to virotherapy. AAV2 has been largely used as a reference serotype for AAV, but we also included AAV6 in our analysis to extend the observations to another AAV serotype. Compared with AAV2, AAV6 produced even faster and larger Ad plaques. AAV6's high capability for airway epithelia transduction is well documented; however, the infectivity of AAV6 in A549 lung adenocarcinoma cells is not superior to AAV2 (Grimm *et al.*, 2008), suggesting that such tropism for lung is not the cause for the AAV6 larger-plaque phenotype. Hence, we focused on serotype 6 for oncolytic studies.

Ad large-plaque phenotype has been associated to enhanced progeny release (Sauthoff *et al.*, 2000; Doronin *et al.*, 2003; Gros *et al.*, 2008). Accordingly, AAV6 enhanced ICOVIR15 release in all cell lines analyzed. However, the time after infection when we detected the highest difference on Ad release induced by AAV was different for each cell line. NP9 showed a delay in this AAV-induced Ad release that could be associated to a lower permissiveness to Ad replication (lower production yields) than A549 and HEK293 cells. In HEK293 and A549 cells, AAV6 decreased Ad production as expected (Carter *et al.*, 1979; Timpe *et al.*, 2006). Moreover, this phenotype was not restricted to an oncolytic Ad, as AAV6 also enhanced Ad5 release. The amount of Ad

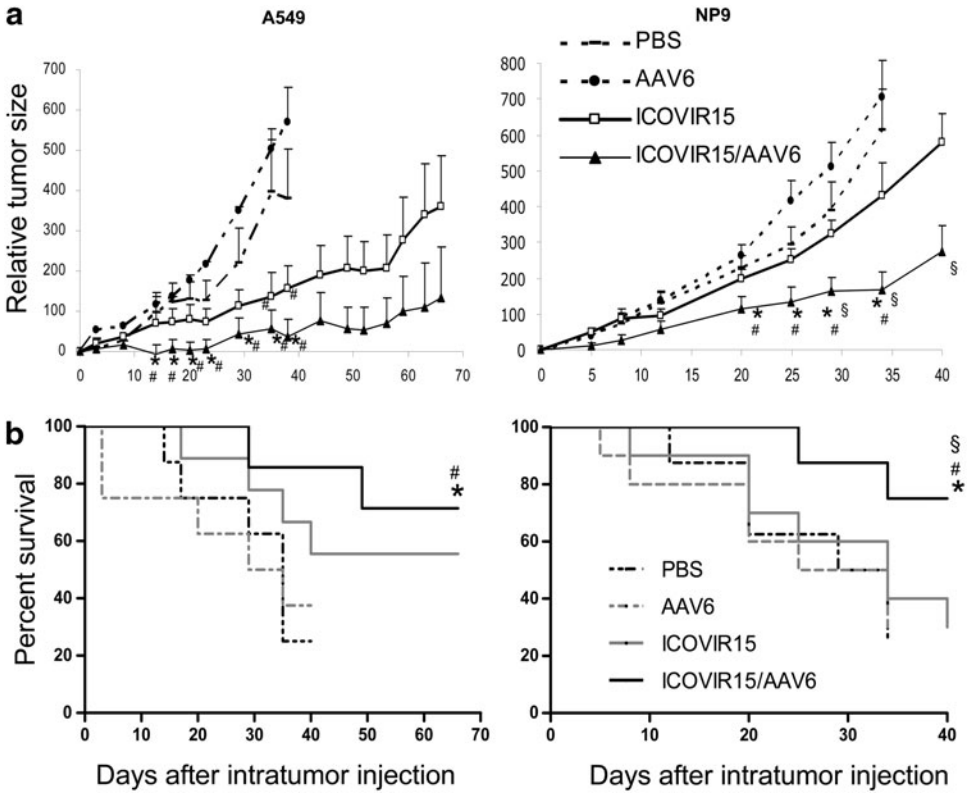

FIG. 4. AAV6 enhances ICOVIR15 antitumor efficacy and prolongs mice survival in two carcinoma tumor xenografts. A549 and NP9 tumor xenografts were treated with a single intratumor dose of PBS, AAV6 (2×10^{10} vp/tumor), ICOVIR15 (2×10^{9} vp/tumor), or a mixture of ICOVIR15 and AAV6 at the same doses. **(a)** Relative tumor growth (percentages of size at treatment, mean ± SE) of 8–10 tumors/group is plotted. $^{*}p \le 0.05$ by two-tailed unpaired Student's *t*-test compared with PBS, $^{\#}p \le 0.05$ by two-tailed unpaired Student's *t*-test compared with AAV6, $^{\S}p \le 0.05$ by two-tailed unpaired Student's *t*-test compared with ICOVIR15. **(b)** Kaplan–Meier survival curves. The end point was established at a tumor volume of $\ge 500\,mm^3$. $^{*}p \le 0.05$ by long-rank test compared with mice injected with PBS, $^{\#}p \le 0.05$ by long-rank test compared with mice injected with AAV6, $^{\S}p \le 0.05$ by long-rank test compared with mice injected with ICOVIR15. PBS, phosphate buffered saline.

present in the total CE immediately after the coincubation time (time point 0) was not influenced by the presence of AAV (Supplementary Fig. S2), suggesting that the AAV's effect on Ad is not associated to initial virus entry.

As Ad is affected by AAV in a dose-dependent manner (Timpe *et al.*, 2006), a range of coinfection conditions with AAV6 were used to evaluate the effects on ICOVIR15 release and total production in A549 cells. Compared with other doses, the dose of 1,000 vp/cell resulted in the highest ratio of released virus to total produced virus and, importantly, in the highest absolute amount of virus in the SN with complete virus release after 48 hr postinfection. Hence, looking only at Ad presence in the SN, the enhanced release overcomes the lower production. We did not find a dose-dependent correlation, as lower or higher doses than 1,000 vp/cell had less impact on virus release.

Several strategies to enhance Ad release have been described: ADP overexpression (Doronin *et al.*, 2003), apoptosis induction by deletion of genes such as *E1B19K* (Sauthoff *et al.*, 2000) or insertion of proapoptotic transgenes (Sauthoff *et al.*, 2002), and bioselection of mutagenized Ads (Subramanian *et al.*, 2006; Gros *et al.*, 2008). ADP overexpression and apoptosis induction accelerate cell death (Sauthoff *et al.*, 2000; Doronin *et al.*, 2003; Subramanian *et al.*, 2006). It has also been observed that AAV induces a characteristic apoptotic cell morphology on Ad-infected cells, with cell shrinkage and membrane blebbing (Timpe *et al.*, 2007). We observed this apoptotic-like morphology (Fig. 3a) as soon as 36 hr after coinfecting with AAV6 at 1,000 vp/cell. This AAV-induced apoptotic-like phenotype correlated to accelerated cell death and cell membrane disruption, which were measured by LDH secretion and trypan blue exclusion. This enhanced cytotoxicity correlates with previous reports of increased cytolysis and apoptosis during the first 3 days after infection of A549 cells with Ad5 and AAV2 (Timpe *et al.*, 2007). However, Jing *et al.* (2001) saw opposite results in HeLa cells that could be related to the different cells used. Our results in A549 and NP9 cells support those of Timpe *et al.* 2007 in favor of an AAV-induced cytotoxicity.

The mechanism whereby AAV increases Ad cytotoxicity is not clear. Here we describe an enhanced release with premature cell death and a characteristic apoptotic-like morphology. Previous reports indicate that AAV Rep proteins induce apoptosis (Zhou and Trempe, 1999; Zhou *et al.*, 1999; Schmidt *et al.*, 2000; Timpe *et al.*, 2007) and that AAV Rep protein expression is inhibited at high AAV doses (Carter *et al.*, 1979; Timpe *et al.*, 2006), decreasing theoretically the proapoptotic effects. In the other hand, adenoviral E1B19K and ADP proteins are related with viral spread, apoptosis, and cytopathic effect (Tollefson *et al.*, 1996a; Subramanian *et al.*, 2006).

From a virotherapy perspective, our aim was to enhance cell lysis, Ad propagation, and antitumor activity of oncolytic Ads. As AAV induced a faster Ad release and increased cytotoxicity, but reduced virus production (burst size), we examined how AAV6 affected ICOVIR15 propagation. With this purpose, propagation-mediated cytotoxicity assays were performed in A549 and NP9 cells using serial virus dilutions (IC_{50} assays). ICOVIR15 propagated faster in the presence of AAV6 at all doses tested. Earlier progeny release is the most obvious explanation for this rapid propagation, increasing the speed of cell-to-cell spread. Using serial dilutions of infected cells, we also observed a significant IC_{50} reduction (11-fold) in both cell lines. The use of coinfected cells is of interest as oncolytic viruses have been administered by carrier cells (Willmon *et al.*, 2009). Our results indicate that the lower Ad yields associated to AAV coinfection are compensated by an earlier release of virus to the SN, and the final outcome is a faster Ad propagation and cytotoxicity (lower IC_{50} values).

To apply our findings to virotherapy, we treated lung and pancreatic adenocarcinomas with a mixture of AAV and oncolytic Ad. It is reported that AAV *per se* can function as a tumor suppressor (Khleif *et al.*, 1991); thus, an AAV-alone treatment was also included. Coinjection with AAV6 improved the antitumor efficacy of ICOVIR15. The faster Ad release and the lower Ad total production, both induced by AAV coinfection, may pose a challenge when attempting to correlate efficacy with intratumoral virus amount by Ad DNA quantification or capsid staining. In fact, we did not find significant differences between intratumor Ad genomes of ICOVIR15/AAV6 and ICOVIR15 groups (data not shown). The strategy to use AAV to foster Ad oncolysis requires coinfection of tumor cells; to maximize it, we used intratumoral administration of a mixture of viruses. Despite that this administration route is commonly used in virotherapy, ideally, systemic administration would be preferred for metastatic cancer. Systemic administration of both viruses would require an AAV biodistribution study in animals bearing tumors after intravenous administration. However, given the limited tumor-targeting capability of Ad, the probability of coinfection of target cells is likely low. Therefore, novel approximations that allow Ad and AAV codelivery should be explored. Use of carrier cells would be an option (Coukos *et al.*, 1999; Garcia-Castro *et al.*, 2005; Hamada *et al.*, 2007). Another strategy could use nonviral vectors carrying infectious plasmids encoding both viruses (Kwon *et al.*, 2011). This strategy is feasible as AAV plasmids are infectious when transfected and plasmids with self-excising Ad genomes have been developed (Stanton *et al.*, 2008).

Our results point that contamination of Ad stocks with AAV could result in enhanced oncolysis, contrary to what could be expected considering only the widely accepted lower Ad yields. Besides the implication that intentional mixing of Ad and AAV may have for efficacy, this observation also raises a caution note on oncolytic Ad potency comparisons, particularly by direct intratumoral administration, as it would require prior AAV detection.

Acknowledgments

We thank María José Castro Castro (Biochemistry Service of Bellvitge Hospital) and Adoración Huertas Ruz and Elisabet Cañete Ortiz (Epigenetic and Cancer Biology Program of the Bellvitge Biomedical Research Institute) for facility and technical support; Juan José Rojas (University of Pittsburgh Cancer Institute, Pittsburg, PA) and Miriam Bazan-Peregrino (Institut d'Investigacions Biomèdiques de Bellvitge, Barcelona, Spain) for extensive revision of this article; and Mercedes Saez (IASIST, S.A.U., Barcelona, Spain) for statistical assistance.

E.L. was supported by a predoctoral fellowship Formación de Profesorado Universitario (FPU) granted by the Spanish Ministry of Education and Science. This work was supported by a grant from the Spanish Ministry of Education and Science (BIO2011-30299-C02-01) and PLE2009-0115 from Spanish Ministry of Economy and Competitivity, and received partial support from the Generalitat de Catalunya (2009SGR284).

Author Disclosure Statement

No competing interests for any of the authors exist.

References

Agrawal, N., *et al.* (2002). Temporal acceleration of the human papillomavirus life cycle by adeno-associated virus (AAV) type 2 superinfection in natural host tissue. Virology 297, 203–210.

Alemany, R. (2007). Cancer selective adenoviruses. Mol. Aspects Med. 28, 42–58.

Carter, B.J., *et al.* (1979). Adeno-associated virus autointerference. Virology 92, 449–462.

Cascallo, M., *et al.* (2007). Systemic toxicity-efficacy profile of ICOVIR-5, a potent and selective oncolytic adenovirus based on the pRB pathway. Mol. Ther. 15, 1607–1615.

Casper, J.M., *et al.* (2005). Identification of an adeno-associated virus Rep protein binding site in the adenovirus E2a promoter. J. Virol. 79, 28–38.

Coukos, G., *et al.* (1999). Use of carrier cells to deliver a replication-selective herpes simplex virus-1 mutant for the intraperitoneal therapy of epithelial ovarian cancer. Clin. Cancer Res. 5, 1523–1537.

Doronin, K., *et al.* (2003). Overexpression of the ADP (E3-11.6K) protein increases cell lysis and spread of adenovirus. Virology 305, 378–387.

Gao, G., *et al.* (2004). Clades of adeno-associated viruses are widely disseminated in human tissues. J. Virol. 78, 6381–6388.

Garcia-Castro, J., *et al.* (2005). Tumor cells as cellular vehicles to deliver gene therapies to metastatic tumors. Cancer Gene Ther. 12, 341–349.

Grimm, D., *et al.* (2003). Preclinical *in vivo* evaluation of pseudotyped adeno-associated virus vectors for liver gene therapy. Blood 102, 2412–2419.

Grimm, D., *et al.* (2008). *In vitro* and *in vivo* gene therapy vector evolution via multispecies interbreeding and retargeting of adeno-associated viruses. J. Virol. 82, 5887–5911.

Gros, A. (2010). Adenovirus release from the infected cell as a key factor for adenovirus oncolysis. Open Gene Ther. J. 3, 24–30.

Gros, A., *et al.* (2008). Bioselection of a gain of function mutation that enhances adenovirus 5 release and improves its antitumoral potency. Cancer Res. 68, 8928–8937.

Hamada, K., *et al.* (2007). Carrier cell-mediated delivery of a replication-competent adenovirus for cancer gene therapy. Mol. Ther. 15, 1121–1128.

Hoggan, M.D., *et al.* (1966). Studies of small DNA viruses found in various adenovirus preparations: physical, biological, and immunological characteristics. Proc. Natl. Acad. Sci. USA 55, 1467–1474.

Jing, X.J., *et al.* (2001). Inhibition of adenovirus cytotoxicity, replication, and E2a gene expression by adeno-associated virus. Virology 291, 140–151.

Khleif, S.N., *et al.* (1991). Inhibition of cellular transformation by the adeno-associated virus rep gene. Virology 181, 738–741.

Kwon, O.J., *et al.* (2011). Viral genome DNA/lipoplexes elicit *in situ* oncolytic viral replication and potent antitumor efficacy via systemic delivery. J. Control Release 155, 317–325.

Muller, O.J., *et al.* (2006). Improved cardiac gene transfer by transcriptional and transductional targeting of adeno-associated viral vectors. Cardiovasc. Res. 70, 70–78.

Puig-Saus, C., *et al.* (2012). Adenovirus i-leader truncation bioselected against cancer-associated fibroblasts to overcome tumor stromal barriers. Mol. Ther. 20, 54–62.

Ramachandra, M., *et al.* (2001). Re-engineering adenovirus regulatory pathways to enhance oncolytic specificity and efficacy. Nat. Biotechnol. 19, 1035–1041.

Rojas, J.J., *et al.* (2010). Minimal RB-responsive E1A promoter modification to attain potency, selectivity, and transgene-arming capacity in oncolytic adenoviruses. Mol. Ther. 18, 1960–1971.

Russell, S.J., *et al.* (2012). Oncolytic virotherapy. Nat. Biotechnol. 30, 658–670.

Sauthoff, H., *et al.* (2000). Deletion of the adenoviral E1b-19kD gene enhances tumor cell killing of a replicating adenoviral vector. Hum. Gene Ther. 11, 379–388.

Sauthoff, H., *et al.* (2002). Late expression of p53 from a replicating adenovirus improves tumor cell killing and is more tumor cell specific than expression of the adenoviral death protein. Hum. Gene Ther. 13, 1859–1871.

Schmidt, M., *et al.* (2000). Adeno-associated virus type 2 Rep78 induces apoptosis through caspase activation independently of p53. J. Virol. 74, 9441–9450.

Schmidt, M., *et al.* (2006). Identification and characterization of novel adeno-associated virus isolates in ATCC virus stocks. J. Virol. 80, 5082–5085.

Stanton, R.J., *et al.* (2008). Re-engineering adenovirus vector systems to enable high-throughput analyses of gene function. Biotechniques 45, 659–662, 664–658.

Subramanian, T., *et al.* (2006). Genetic identification of adenovirus type 5 genes that influence viral spread. J. Virol. 80, 2000–2012.

Timpe, J.M., *et al.* (2006). Effects of adeno-associated virus on adenovirus replication and gene expression during coinfection. J. Virol. 80, 7807–7815.

Timpe, J.M., *et al.* (2007). Adeno-associated virus induces apoptosis during coinfection with adenovirus. Virology 358, 391–401.

Tollefson, A.E., *et al.* (1996a). The E3-11.6-kDa adenovirus death protein (ADP) is required for efficient cell death: characterization of cells infected with adp mutants. Virology 220, 152–162.

Tollefson, A.E., *et al.* (1996b). The adenovirus death protein (E3-11.6K) is required at very late stages of infection for efficient cell lysis and release of adenovirus from infected cells. J. Virol. 70, 2296–2306.

Villanueva, A., *et al.* (1998). Disruption of the antiproliferative TGF-beta signaling pathways in human pancreatic cancer cells. Oncogene 17, 1969–1978.

Wein, L.M., *et al.* (2003). Validation and analysis of a mathematical model of a replication-competent oncolytic virus for cancer treatment: implications for virus design and delivery. Cancer Res. 63, 1317–1324.

Willmon, C., *et al.* (2009). Cell carriers for oncolytic viruses: Fed Ex for cancer therapy. Mol. Ther. 17, 1667–1676.

Zhou, C., and Trempe, J.P. (1999). Induction of apoptosis by cadmium and the adeno-associated virus Rep proteins. Virology 261, 280–287.

Zhou, C., *et al.* (1999). Enhancement of UV-induced cytotoxicity by the adeno-associated virus replication proteins. Biochim. Biophys. Acta 1444, 371–383.

Zolotukhin, S., *et al.* (1999). Recombinant adeno-associated virus purification using novel methods improves infectious titer and yield. Gene Ther. 6, 973–985.

Address correspondence to:
Dr. Ramon Alemany
Translational Research Laboratory
IDIBELL-Institut Català d'Oncologia
Av Gran Via de l'Hospitalet 199-203
L'Hospitalet de Llobregat
08907 Barcelona
Spain

E-mail: ralemany@iconcologia.net

Received for publication August 7, 2013;
accepted after revision September 9, 2013.

Published online: September 10, 2013.